ucd-tpg:1103.04

Massless Dirac Fermions in Electromagnetic Field

Ahmed Jellal[a,b,c*], **Abderrahim El Mouhafid**[b,c] and **Mohammed Daoud**[d,e]

[a] *Physics Department, College of Sciences, King Faisal University, PO Box 380, Alahsa 31982, Saudi Arabia*

[b] *Saudi Center for Theoretical Physics, Dhahran, Saudi Arabia*

[c] *Theoretical Physics Group, Faculty of Sciences, Chouaïb Doukkali University, PO Box 20, 24000 El Jadida, Morocco*

[d] *Max Planck Institute for the Physics of Complex Systems, 01187 Dresden, Germany*

[e] *Department of Physics, Faculty of Sciences, Ibn Zohr University, PO Box 8106, 80006 Agadir, Morocco*

arXiv:1103.5297v2 [hep-th] 12 Feb 2012

Abstract

We study the relations between massless Dirac fermions in an electromagnetic field and atoms in quantum optics. After getting the solutions of the energy spectrum, we show that it is possible to reproduce the 2D Dirac Hamiltonian, with all its quantum relativistic effects, in a controllable system as a single trapped ion through the Jaynes–Cummings and anti-Jaynes–Cummings models. Also we show that under certain conditions the evolution of the Dirac Hamiltonian provides us with Rashba spin-orbit and linear Dresselhaus couplings. Considering the multimode multiphoton Jaynes-Cummings model interacting with N modes of electromagnetic field prepared in general pure quantum states, we analyze the Rabi oscillation. Evaluating time evolution of the Dirac position operator, we determine the Zitterbewegung frequency and the corresponding oscillating term as function of the electromagnetic field.

*ajellal@ictp.it - jellal.a@ucd.ca.ma

1 Introduction

In graphene [1, 2, 3], the linear electronic band dispersion near the Dirac points gave rise to charge carriers (electrons or holes) that propagate as if they were massless fermions with speeds of the order of $10^6 m/s$ rather than the speed of light $3 \times 10^8 m/s$. Hence, charge carriers in this structure should be described by the massless Dirac equation rather than the usual Schrödinger equation. The physics of relativistic electrons is thus now experimentally accessible in graphene based solid-state devices, whose behavior differs drastically from that of similar devices fabricated with usual semiconductors. Consequently, new unexpected phenomena have been observed while other phenomena that were well-understood in common semiconductors, such as the quantum Hall effect [4, 5]. Thus, graphene devices enabled the study of relativistic dynamics in controllable nano-electronic circuits (relativistic electrons on-a-chip) and their behavior probes our most basic understanding of electronic processes in solids. It also allowed to establish a relationship between massless Dirac fermions in two dimensions and quantum optics, for instance one can see [6, 7].

On the other hand, Jaynes–Cummings (JC) model is describing the basic interaction of a two-level atom and quantized field, which is also the cornerstone for the treatment of the interaction between light and matter in quantum optics [8]. It can be used to explain many quantum phenomena, such as the collapses and revivals of the atomic population inversions, squeezing of the quantized field and the atom-cavity entanglement. Recent experiments showed that JC model can be implicated in quantum-state engineering and quantum information processing, e.g. generation of Fock states [9] and entangled states [10], and the implementations of quantum logic gates [11], etc. Originally, JC model is physically implemented with a cavity quantum electrodynamics system, see for instance [12]. Certainly, there has been also interest to realize JC model with other physical systems. A typical system is a cold ion trapped in a Paul trap and driven by classical laser beams [13, 14] where the interaction between two selected internal electronic levels and the external vibrational mode of the ion can be induced.

The relationship between the relativistic systems and atoms in quantum optics is studied for differen purposes. With this respect, the first theoretical proposal was done by Lamata *et al.* [15] and its experimental realization was done by Gerritsma *et al.* [16]. Subsequently, different progresses appreared on the subject [17, 18, 19, 20] where for example in [20], the dynamics of the 2+1 Dirac oscillator exactly was studied and spin oscillations due to a Zitterbewegung of purely relativistic origin was found. An exact mapping of this quantum-relativistic system onto a JC model is established. This equivalence allowed to map a series of quantum optical phenomena onto the relativistic oscillator and vice versa. A realistic experimental proposal was made, in reach with current technology, for studying the equivalence of both models using a single trapped ion.

Motivated by different developments and in particular [15, 20], we consider massless Dirac fermions in an electromagnetic field and show its link with JC and anti-Jaynes–Cummings (AJC) models. This can be done by determining the solutions of the energy spectrum and mapping the corresponding eigenspinors in terms of two states of JC model. Furthermore, we analyze the Rabi oscillations by considering atoms coupled to the field states and evolve in time according to the stationary eigenspinors. This allows us to obtain two normalization coefficients in terms of the Rabi frequency, which verify the normalization condition. By evaluating the probabilities of the atom in the ground and ex-

cited states, we show that the probability predicts sinusoidal Rabi oscillations, much like the classical case, and exists even when the field is initially in the ground state.

Finally, we deal with another aspect of Dirac fermions in graphene [21, 22, 23] that is the Zitterbewegung (ZB) effect. Indeed, by calculating time evolution of the Dirac position operator, we end up with an extra term. After inspection, we show that this term represents a quantum oscillation about the classical motion and indicates the existence of the ZB effect. By evaluating the expectation value of the Dirac position, we obtain the ZB frequency in terms of the energy levels and magnetic field, which disappears for a null energy.

The present paper is organized as follows. In section 2, we consider the Hamiltonian describing one massless Dirac fermion in electromagnetic field with Zeeman effect. By choosing the Landau gauge, we obtain the eigenvalues and the corresponding eigenspinors. After setting different ingredients, we establish the link between our system and quantum optics through JC and AJC models in section 3. The Rabi oscillations for atoms coupled to field states in graphene will be analyzed in section 4. Using the Heisenberg picture dynamics we study the ZB effect and determine its oscillation frequency in section 5. Finally we close our work by concluding and giving some perspectives.

2 Dirac fermions in electromagnetic field

In graphene, the two Fermi points, each with a two-fold band degeneracy, can be described by a low-energy continuum approximation with a four-component envelope wavefunction whose components are labeled by a Fermi-point pseudospin $= \pm 1$ and a sublattice forming an honeycomb. Under this approximation we can describe our charge carriers, in electromagnetic field $(\vec{E}, \vec{B})$ where $\vec{E} = E\vec{e}_y$, by a gauge invariant Dirac Hamiltonian in 2+1 space-time dimensions with minimal coupling to the vector potential and Zeeman effect as follows

$$H_D = v_F \vec{\sigma} \cdot \vec{\pi} + \sigma_y eEy + \frac{1}{2} g\mu_B B\sigma_z \tag{1}$$

where $v_F \approx 10^6 m/s$ is the Fermi velocity, the conjugate momentum is $\vec{\pi} = \vec{p} - \frac{e}{c}\vec{A}$, g is the Landé factor, μ_B is the Bohr magneton, $\vec{\sigma}$ are Pauli spin matrices and the nonzero matrix elements of σ_z are $\langle\uparrow|\ \sigma_z\ |\uparrow\rangle = +1$ and $\langle\downarrow|\ \sigma_z\ |\downarrow\rangle = -1$. Choosing the vector potential in the Landau gauge $\vec{A}(x, y) = (-By, 0)$ to write (1) as

$$H_D = v_F \begin{pmatrix} 0 & p_x - ip_y - \frac{eB}{c}y - i\frac{eE}{v_F}y \\ p_x + ip_y - \frac{eB}{c}y + i\frac{eE}{v_F}y & 0 \end{pmatrix} + \frac{1}{2} g\mu_B B\sigma_z. \tag{2}$$

By setting $\xi = 1 + i\frac{cE}{v_F B}$ and $\bar{\xi} = 1 - i\frac{cE}{v_F B}$, we obtain the form

$$H_D = v_F \begin{pmatrix} 0 & p_x - ip_y - \frac{\hbar}{l_B^2}\ \xi y \\ p_x + ip_y - \frac{\hbar}{l_B^2}\ \bar{\xi} y & 0 \end{pmatrix} + \frac{1}{2} g\mu_B B\sigma_z \tag{3}$$

where $l_B = \sqrt{\frac{\hbar c}{eB}}$ is the magnetic length.

To diagonalize the above Hamiltonian, it is convenient to introduce the annihilation and creation operators. They are

$$a = \frac{l_B}{\hbar\sqrt{2}} \left(ip_x - p_y - i\frac{\hbar}{l_B^2}\xi y \right), \qquad a^\dagger = \frac{l_B}{\hbar\sqrt{2}} \left(-ip_x - p_y + i\frac{\hbar}{l_B^2}\bar{\xi} y \right) \tag{4}$$

which satisfy the commutation relation

$$\left[a^{\dagger}, a\right] = \mathbb{I}. \tag{5}$$

These can be used to write H_D as

$$H_D = \begin{pmatrix} \frac{1}{2}g\mu_B B & i\hbar\omega_c a^{\dagger} \\ -i\hbar\omega_c a & -\frac{1}{2}g\mu_B B \end{pmatrix} \tag{6}$$

where we have set the frequency $\omega_c = \sqrt{2}\frac{v_F}{l_B}$.

The complete solutions of the energy spectrum can be obtained by solving the time independent Dirac equation $H_D\phi = \varepsilon\phi$. Note that, the form of our Hamiltonian suggests to separate variables by writing the eigenspinors as

$$\phi(x,y) = \chi(x)\psi(y), \qquad \psi(y) = (\psi_1, \psi_2)^t, \qquad \chi(x) = e^{ik_x x} \tag{7}$$

with k_x is a real parameter that stands for the wave number of the excitations along x-direction. Thus, the reduced eigenvalue equation is given by

$$H_D \begin{pmatrix} \mid \psi_1\rangle \\ \mid \psi_2\rangle \end{pmatrix} = \varepsilon \begin{pmatrix} \mid \psi_1\rangle \\ \mid \psi_2\rangle \end{pmatrix} \tag{8}$$

which leads to the relations

$$i\hbar\omega_c a^{\dagger} \mid \psi_2\rangle = \left(\varepsilon - \frac{1}{2}g\mu_B B\right) \mid \psi_1\rangle \tag{9}$$

$$-i\hbar\omega_c a \mid \psi_1\rangle = \left(\varepsilon + \frac{1}{2}g\mu_B B\right) \mid \psi_2\rangle. \tag{10}$$

As we will see soon these will be solved by making separation between the positive and negative energy solutions as well as discussing the relation between them.

The positive energy solution can be obtained from (9) and (10) to get the following relation between spinor components

$$\mid \psi_2\rangle = \frac{-i\hbar\omega_c}{\left(\varepsilon + \frac{1}{2}g\mu_B B\right)} a \mid \psi_1\rangle. \tag{11}$$

Clearly, it is necessary to impose the condition $\varepsilon \neq -\frac{1}{2}g\mu_B B < 0$, which tells us that (11) is valid only for positive energies corresponding to the positive eigenspinors denoted by $\mid \psi^{+}\rangle = \begin{pmatrix} \mid \psi_1^{+}\rangle \\ \mid \psi_2^{+}\rangle \end{pmatrix}$. Now, from (11) we show that $\mid \psi_1^{+}\rangle$ satisfies the second differential equation

$$\left[\varepsilon^2 - \left(\frac{1}{2}g\mu_B B\right)^2 - \hbar^2\omega_c^2 a^{\dagger}a\right] \mid \psi_1^{+}\rangle = 0 \tag{12}$$

which is nothing but a simple harmonic oscillator type. Thus, the positive eigenvalues are given by

$$\varepsilon_n^{+} = +\sqrt{\hbar^2\omega_c^2 n + \frac{1}{4}(g\mu_B B)^2}, \qquad n = 0, 1, 2, \cdots \tag{13}$$

where the corresponding eigenstates take the form

$$\mid \psi_1^{+}\rangle = \mid n\rangle = \frac{\left(a^{\dagger}\right)^n}{\sqrt{n!}} \mid 0\rangle. \tag{14}$$

At this level, it is interesting to mention that these eigenstates are clearly depending on the electromagnetic field. To clarify this statement, we write them as

$$\mid \psi_1^+\rangle = \frac{(-il_B)^n}{\sqrt{2^n n!}} \left(k_x + \partial_y - \frac{\hbar}{l_B^2}\bar{\xi} y \right)^n \mid 0\rangle \tag{15}$$

with k_x is the wave vector along x-direction and the parameter $\bar{\xi} = 1 - i\frac{cE}{v_F B}$ is a function of the ratio between the two fields. Now inserting (14) into (11) to find

$$\mid \psi_2^+\rangle = \frac{-i\hbar\omega_c}{\varepsilon_n^+ + \frac{1}{2}g\mu_B B} a \mid n\rangle = -i\sqrt{\frac{\varepsilon_n^+ - \frac{1}{2}g\mu_B B}{\varepsilon_n^+ + \frac{1}{2}g\mu_B B}} \mid n-1\rangle. \tag{16}$$

Combining all, we write the eigenspinors as

$$\mid \psi_n^+\rangle = \begin{pmatrix} u_n^+ \mid n\rangle \\ -iu_n^- \mid n-1\rangle \end{pmatrix} \tag{17}$$

where the amplitude $u_n^\pm$ read as

$$u_n^\pm = \left(\frac{1}{2} \pm \frac{\frac{1}{4}g\mu_B B}{\sqrt{\hbar^2\omega_c^2 n + \frac{1}{4}(g\mu_B B)^2}} \right)^{\frac{1}{2}}. \tag{18}$$

As far as the negative energy solution is concerned, we use similar approach to end up with the eigenvalues

$$\varepsilon_m^- = -\sqrt{\hbar^2\omega_c^2(m+1) + \frac{1}{4}(g\mu_B B)^2}, \qquad m = 0, 1, 2, \cdots. \tag{19}$$

To derive the corresponding negative eignespinors, we use the energy conservation

$$(\varepsilon_n^+)^2 = (\varepsilon_m^-)^2 \tag{20}$$

which tells us that the two quantum numbers are related by $n = m + 1$. Thus, we obtain

$$\mid \psi_n^-\rangle = \begin{pmatrix} +iu_n^+ \mid n+1\rangle \\ u_n^- \mid n\rangle \end{pmatrix} \tag{21}$$

where $u_n^\pm$ are given in (18). We recall that all eigenspinors obtained so far are electromagnetic field $(\vec{E}, \vec{B})$ dependent.

For later use, it is convenient to write the eigenspinors (17) and (21) in an appropriate form. This can be done by using the Pauli spinors, such as

$$\mid \psi_n^+\rangle \equiv \mid \psi_{n,\sigma,\varepsilon_n^+}\rangle \;\; = \;\; u_n^+ \mid n,\uparrow\rangle - iu_n^- \mid n-1,\downarrow\rangle \tag{22}$$

$$\mid \psi_n^-\rangle \equiv \mid \psi_{n,\sigma,\varepsilon_n^-}\rangle \;\; = \;\; u_n^- \mid n,\uparrow\rangle + iu_n^+ \mid n-1,\downarrow\rangle. \tag{23}$$

This summarizes the obtained results so far, which will be employed to study different issues in the forthcoming anaylsis. More precisely, we will implement them to establish a link between massless Dirac Fermions in electromagnetic field and atoms in quantum optics. Subsequentely, we will discuss the possibility to make contact with the Rabi oscillations and ZB effect as well.

3 Link with Jaynes–Cummings models

As claimed before, we would like to use our results in order to make contact with quantum optic systems through two relevant models, i.e. JC and AJC. In doing so, first let us prepare our system to make the required contact easy and clear. From (9) and (10) we show that the Hamiltonian (6) takes the form

$$H_D = i\hbar\omega_c \left(a^\dagger \mid \psi_2\rangle\langle\psi_1 \mid -a \mid \psi_1\rangle\langle\psi_2 \mid \right) + \frac{1}{2} g\mu_B B\sigma_z \tag{24}$$

which can easily be written as

$$H_D = \hbar \left(g'\sigma^- a^\dagger + g'^*\sigma^+ a \right) + \frac{1}{2} g\mu_B B\sigma_z. \tag{25}$$

This Hamiltonian can be interpreted as a model of quantum optics where $g' = i\omega_c$ is the coupling strength between the atom and electromagnetic field, σ^+ and σ^- are the spin raising and lowering operators, respectively. More precisely, (25) is describing a single two-state atom, represented by the Pauli matrices, interacting with a (single-mode quantized) electromagnetic field. This statement will be clarified in the next.

We will show how to implement the dynamics of (25) in a single ion inside a Paul trap with two frequencies ν_x and ν_y. For this, let us consider a system of two-level atom of the ground $\mid e\rangle$ and excited $\mid f\rangle$ states where the eigenspinors (17) can be split into

$$\mid \psi\rangle = \mid \psi_1\rangle \mid e\rangle + \mid \psi_2\rangle \mid f\rangle. \tag{26}$$

These two metastable internal states $\mid e\rangle$ and $\mid f\rangle$ are corresponding to the following energies

$$\varepsilon_{n_e} = \hbar\omega_{n_e} = \hbar\sqrt{\omega_c^2 n_e + (1/2g\mu_B B/\hbar)^2}, \qquad \varepsilon_{n_f} = \hbar\omega_{n_f} = \sqrt{\omega_c^2 n_f + (1/2g\mu_B B/\hbar)^2} \tag{27}$$

where the energy difference between them is characterized by the transition frequency $\omega_0 = \left(\varepsilon_{n_e} - \varepsilon_{n_f}\right)/\hbar$. All observable quantities of this two-state system can be conveniently represented by the Pauli operators, such as

$$\sigma_z = \mid e\rangle\langle e \mid - \mid f\rangle\langle f \mid, \qquad \sigma^+ = \mid e\rangle\langle f \mid, \qquad \sigma^- = \mid f\rangle\langle e \mid \tag{28}$$

where the expectation value of the operator σ_z is the atomic inversion, while σ^+ and σ^- induce upward and downward transition respectively. It is sometimes convenient to work with the Hermitian combinations of σ^+ and σ^-, i.e. $\sigma_x = \sigma^+ + \sigma^-$ and $\sigma_y = i(\sigma^+ - \sigma^-)$. Using these to write the Hamiltonian (25) as

$$H_D = \upsilon_F \left(\sigma_x p_x + \sigma_y p_y\right) + \frac{\hbar\omega_c}{\sqrt{2}l_B} \left(-\sigma_x + \frac{cE}{B}\sigma_y \right) y + \frac{1}{2} g\mu_B B\sigma_z \tag{29}$$

which is showing its dependence on the electric field through the extra term $\frac{cE}{B}\sigma_y$ appearing in the Hamiltonian form. Clearly for $E = 0$, one recovers a system of massless Dirac fermions in magnetic field and thus the extra term can be seen as a shift to the spin σ_x. Certainly, this will play a crucial role in the forthcoming analysis and make difference with respect to the former results obtained in this direction [20].

Having set all ingredients, let us show that the Dirac Hamiltonian (29) can be linked with JC and AJC models. We start by introducing JC model, usually called red-sideband excitation, which is consisting of a laser field acting resonantly on two internal levels. Typically, a resonant JC coupling induces an excitation in the internal levels while producing a deexcitation of the motional harmonic oscillator and viceversa. The resonant JC Hamiltonian is given by

$$H_i^{JC} = \hbar\eta_i\Omega_i\left(\sigma^+ a_i e^{i\phi} + \sigma^- a_i^+ e^{-i\phi}\right) + \hbar\delta_i\sigma_z \tag{30}$$

where a_i and a_i^+ $(i = x, y)$ are the annihilation and creation operators associated with a motional degree of freedom. $\eta_i := k_i\sqrt{\hbar/2M\nu_i}$ is the Lamb-Dicke parameter [14], k_i is the wave number of the driving field, M is the ion mass, ν_i are the natural trap frequencies, ϕ is the red-sideband phase, Ω_i and δ_i are the excitation coupling strengths. Using the realization (4) for the annihilation and creation operators to map (30) as

$$\begin{aligned} H_i^{JC} &= \frac{\eta_i\Omega_i l_B}{\sqrt{2}}\left[i(\sigma^+e^{i\phi} - \sigma^-e^{-i\phi})p_x - (\sigma^+e^{i\phi} + \sigma^-e^{-i\phi})p_y\right] \\ &\quad + \frac{\hbar\eta_i\Omega_i}{\sqrt{2}l_B}\left[-i(\sigma^+e^{i\phi} - \sigma^-e^{-i\phi}) - \frac{cE}{B}(\sigma^+e^{i\phi} + \sigma^-e^{-i\phi})\right] y + \hbar\delta_i\sigma_z. \end{aligned} \tag{31}$$

On the other hand, the AJC Hamiltonian reads as

$$H_i^{AJC} = \hbar\eta_i\Omega_i\left(\sigma^+ a_i^+ e^{i\varphi} + \sigma^- a_i e^{-i\varphi}\right) \tag{32}$$

where φ is the blue-sideband phase. In similar way to (30), we show that H_i^{AJC} takes the form

$$\begin{aligned} H_i^{AJC} &= \frac{\eta_i\Omega_i l_B}{\sqrt{2}}\left[-i(\sigma^+e^{i\varphi} - \sigma^-e^{-i\varphi})p_x - (\sigma^+e^{i\varphi} + \sigma^-e^{-i\varphi})p_y\right] \\ &\quad + \frac{\hbar\eta_i\Omega_i}{\sqrt{2}l_B}\left[i(\sigma^+e^{i\varphi} - \sigma^-e^{-i\varphi}) - \frac{cE}{B}(\sigma^+e^{i\varphi} + \sigma^-e^{-i\varphi})\right] y. \end{aligned} \tag{33}$$

By fixing different parameters, let us see how does look like the sum of $H_i^{JC} + H_i^{AJC}$. Indeed, for particular values of the involved parameters we obtain table 1:

i	δ_i	ϕ	φ	$H_i^{JC} + H_i^{AJC}$
x	δ	$\frac{3\pi}{2}$	$\frac{\pi}{2}$	$\sqrt{2}\eta\Omega l_B\sigma_x p_x + \hbar\delta\sigma_z$
y	0	$\frac{3\pi}{2}$	$\frac{3\pi}{2}$	$\sqrt{2}\eta\Omega l_B\sigma_y p_y + \frac{\sqrt{2}\hbar\eta\Omega}{l_B}\frac{cE}{B}\sigma_y y$
y	0	$\frac{3\pi}{2}$	$\frac{\pi}{2}$	$-\frac{\sqrt{2}\hbar\eta\Omega}{l_B}\sigma_x y$

Table 1: Linear combinations of JC and AJC Hamiltonian's for given values of the involved parameters.

Now by summing all terms in table 1, one gets

$$\sum_i\left(H_i^{JC} + H_i^{AJC}\right) = \sqrt{2}\eta\Omega l_B\left(\sigma_x p_x + \sigma_y p_y\right) + \frac{\sqrt{2}\hbar\eta\Omega}{l_B}\left(-\sigma_x + \frac{cE}{B}\sigma_y\right) y + \hbar\delta\sigma_z. \tag{34}$$

A comparison to the Dirac Hamiltonian (29) yields to the following correspondence

$$\begin{cases} \omega_c := 2\eta\Omega \\ \frac{1}{2}g\mu_B B := \hbar\delta \end{cases} \tag{35}$$

where $\Omega = \Omega_i$ and $\eta = \eta_i$, $\forall i = x, y$. (35) means that if the Lamb-Dicke parameter η is restricted to the ratio between the cyclotron frequency ω_c and the excitation coupling strength Ω supplemented by a variation of magnetic field like the excitation coupling strength δ, then the present system can be linked with the atoms in quantum optics. Otherwise, (35) tells us that it is possible to reproduce the 2D Dirac Hamiltonian (29), with all its quantum relativistic effects, in a controllable system as a single trapped ion. This conclusion is deduced also by analyzing massive Dirac fermions in magnetic field in the same framework [20].

We close this section by showing that the system under consideration can be reduced to spintronic ones. In doing so, let us choose different parameters as summarized in table 2:

i	δ	ϕ	φ	$H_i^{JC} + H_i^{AJC}$
x	δ	0	π	$\sqrt{2}\eta\Omega l_B \sigma_y p_x + \hbar\delta\sigma_z$
y	0	0	0	$-\sqrt{2}\eta\Omega l_B \sigma_x p_y - \frac{\sqrt{2}\hbar\eta\Omega}{l_B}\frac{cE}{B}\sigma_x y$

Table 2: Configuration of four parameters leading to new form of $H_i^{JC} + H_i^{AJC}$.

Summing over i to obtain the Hamiltonian

$$\sum_i \left(H_i^{JC} + H_i^{AJC}\right) = \sqrt{2}\eta\Omega l_B \left(\sigma_y p_x - \sigma_x p_y\right) - \frac{\sqrt{2}\hbar\eta\Omega}{l_B}\frac{cE}{B}\sigma_x y + \hbar\delta\sigma_z. \tag{36}$$

By taking $E = 0$ and $\delta = 0$ in (36), the resulted term is nothing but the Rashba spin-orbit coupling [24] where the coefficient $\sqrt{2}\eta\Omega l_B$ is identified to the coupling parameter of Rashba type.

One can ask for other configurations of the involved parameters and see what we gain. Indeed, let us take the choice listed in table 3:

i	δ	ϕ	φ	$H_i^{JC} + H_i^{AJC}$
x	δ	$\frac{3\pi}{2}$	$\frac{\pi}{2}$	$\sqrt{2}\eta\Omega l_B \sigma_x p_x + \hbar\delta\sigma_z$
y	0	$\frac{\pi}{2}$	$\frac{\pi}{2}$	$-\sqrt{2}\eta\Omega l_B \sigma_y p_y - \frac{\sqrt{2}\hbar\eta\Omega}{l_B}\frac{cE}{B}\sigma_y y$

Table 3: Configuration of four parameters leading to new form of $H_i^{JC} + H_i^{AJC}$.

As before we sum up to obtain the Hamiltonian

$$\sum_i \left(H_i^{JC} + H_i^{AJC}\right) = \sqrt{2}\eta\Omega l_B \left(\sigma_x p_x - \sigma_y p_y\right) - \frac{\sqrt{2}\hbar\eta\Omega}{l_B}\frac{cE}{B}\sigma_y y + \hbar\delta\sigma_z \tag{37}$$

which reduces to the linear Dresselhaus coupling [24] for $E = 0$ and $\delta = 0$. According to (36) and (37), one can conclude that the system under consideration is also sharing some features with spintronic systems. Therefore one can go further to investigate the basic features of (36) and (37) to extract more information about these relationships.

4 Rabi oscillations

The Rabi oscillations of fermions in graphene have been studied in different contexts to deal with some issues [6, 7]. For example in [6] the relation between the canonical model of quantum optics, JC model

and Dirac fermions in quantizing magnetic field was investigated. It was demonstrated that Rabi oscillations are observable in the optical response of graphene, providing with a transparent picture about the structure of optical transitions. While the longitudinal conductivity reveals chaotic Rabi oscillations, the Hall component measures coherent ones. This opens up the possibility of investigating a microscopic model of a few quantum objects in a macroscopic experiment with tunable parameters.

Motivated by the above developments, we analyze the Rabi oscillations of the system under consideration. We start by expanding a general state on to the obtained eigenspinors (17) to study the corresponding dynamics. Let us assume that initially at $t = 0$ the atom is in the lower state $\mid f\rangle$ and the cavity contains precisely $n-1$ photons, i.e. the field is in a number (Fock) state $\mid n-1\rangle$ with $n = 1, 2, \cdots$. Then the initial state of the system is $\mid f, n-1\rangle$, while the interaction term of the Hamiltonian (25) connects this initial state to the final state $\mid e, n\rangle$. To proceed further, we consider the initial state for the field as $\mid \psi(0)\rangle = \mid f, n-1, \downarrow\rangle$ and assume an atom in the excited state is injected into the field. Using (22), (23) and (26), one can write the initial state as

$$\mid \psi(0)\rangle = iu_n^- \mid \psi_{n,\sigma,\varepsilon_n^+}\rangle - iu_n^+ \mid \psi_{n,\sigma,\varepsilon_n^-}\rangle. \tag{38}$$

Its evolution state can easily be obtained by acting as

$$\mid \psi(t)\rangle = e^{-\frac{i}{\hbar}H_D t} \mid \psi(0)\rangle = C_{e,n}(t) \mid e, n, \uparrow\rangle + C_{f,n-1}(t) \mid f, n-1, \downarrow\rangle \tag{39}$$

where the coefficients are given by

$$C_{e,n}(t) = \sqrt{\frac{4\zeta n}{1+4\zeta n}} \sin(\omega_n t) \tag{40}$$

$$C_{f,n-1}(t) = \cos(\omega_n t) + \frac{i}{\sqrt{1+4\zeta n}} \sin(\omega_n t). \tag{41}$$

It is easy to check that they verify the normalization condition $|C_{e,n}(t)|^2 + |C_{f,n-1}(t)|^2 = 1$. The frequency of oscillations is given by

$$\omega_n := \frac{E_n}{\hbar} = \delta\sqrt{1+4\zeta n} \tag{42}$$

where the parameter $\zeta = \left(\frac{\omega_c}{2\delta}\right)^2$ controls the nonrelativistic limit. (39) shows very clearly the non-stationary states of localization ($\mid e, n, \uparrow\rangle$, $\mid f, n-1, \downarrow\rangle$), which is nothing but the Rabi oscillation that is a simple quantum beat interstate $\mid e, n, \uparrow\rangle$ and $\mid f, n-1, \downarrow\rangle$. Moreover, the dynamics of (39) is completely similar to the atomic Rabi oscillations that can be seen from the JC model. This similarity shows another way how the system under consideration can be linked with Rabi oscillations.

To understand better the present situation, let us analyze the probabilities of existence. Indeed, for a atom in the state $\mid f, n-1, \downarrow\rangle$, we find

$$P_{n-1}^f(t) = 1 - \frac{4\xi n}{1+4\xi n} \sin^2(\omega_n t) = 1 - \left(1 - \frac{\delta^2}{\omega_n^2}\right) \sin^2(\omega_n t) \tag{43}$$

where ω_n is now identified to the Rabi frequency ω_R. It is clear that, $P_{n-1}^f(t)$ oscillates between a maximum of unity and a minimum of $\left(\frac{\delta}{\omega_n}\right)^2$. (43) predicts sinusoidal Rabi oscillations much like the

classical case. However, even when the field is initially in vacuum state, i.e. $n = 0$, the probability exists.

Now let see what happens when the atom is in the state $\mid e, n, \downarrow\rangle$. Indeed, after some algebra we get the probability

$$P_n^e(t) = \frac{4\zeta n}{1+4\zeta n}\sin^2(\omega_R t) = \left(1 - \frac{\delta^2}{\omega_R^2}\right)\sin^2(\omega_R t). \tag{44}$$

This can be plotted as shown in Figure 1 for some particular value of δ. One can easily notices that for the resonance case ($\delta = 0$), $P_n^e(t)$ reduces to

$$P_n^e(t) = \sin^2(\omega_R t) \tag{45}$$

which is in agreement with blue figure (Figure 1). For $t = \pi/2\omega_R$ all the atomic population has been transferred to the excited state. Clearly, the probabilities $P_n^e(t)$ and $P_{n-1}^f(t)$ oscillate in time with the Rabi frequency ω_R where their amplitude are maximum at $\delta = 0$ and decrease rapidly as δ increases. Contrary, in a stationary state the probabilities of localization of the particle are equal and constant.

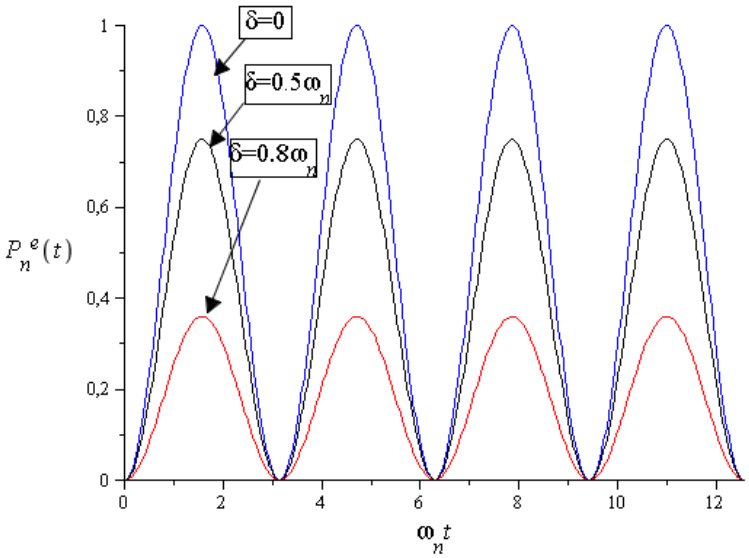


Figure 1: Plots of $P_n^e(t)$ versus t for various detunings δ.

It is frequently convenient to consider the atomic inversion $W(t)$, which is defined as the difference in the excited and ground state populations. This is

$$W(t) = P_n^e(t) - P_{n-1}^f(t) = 2\left(1 - \frac{\delta^2}{\omega_R^2}\right)\sin^2(\omega_R t) - 1 \tag{46}$$

which can be simplified by assuming that the atom is initially in the ground state and requiring the resonant case. These allow us to obtain

$$W(t) = \sin^2(\omega_R t) - \cos^2(\omega_R t) = -\cos(2\omega_R t) \tag{47}$$

where the Rabi frequency reduces now to the quantity $\omega_R = \sqrt{n}\omega_c$. Again, for $t = \pi/2\sqrt{n}\omega_c$ all the population is transferred to the excited state and we have $W(\pi/2\sqrt{n}\omega_c) = 1$. On the other hand, if

we choose $t = \pi/4\sqrt{n}\omega_c$, then $W(\pi/4\sqrt{n}\omega_c) = 0$ and the population is shared coherently between the excited and ground states. This case shows the constraint

$$C_{e,n}(\pi/4\sqrt{n}\omega_c) = C_{f,n-1}(\pi/4\sqrt{n}\omega_c) = \frac{1}{\sqrt{2}} \tag{48}$$

and therefore the corresponding state is

$$|\psi(\pi/4\sqrt{n}\omega_c)\rangle = \frac{1}{\sqrt{2}}\left(|e, n, \uparrow\rangle + |f, n-1, \downarrow\rangle\right). \tag{49}$$

In summary, one can see that the behavior of two-level atom interacting with a single electromagnetic mode is surprisingly rich. In fact, there are Rabi oscillations that collapse and remain quiescent, revive, then collapse again.

5 Zitterbewegung effect

The Zitterbewegung (ZB) effect, called also trembling motion, is consisting of a helicoidal motion of a free Dirac particle. It is a natural consequence of the non-commutativity of its velocity operator components $v_F\vec{\sigma}_j$, with $i = x, y$. In connection with quantum optics realm, this quantum relativistic effect was studied by Lamata *et al.* [15]. The ZB effect has been also studied for different reasons in systems made of graphene [21, 22, 23]. For instance in [22], the electric current and spatial displacement due the ZB effect of electrons in graphene in the presence of an external magnetic field were described. It was shown that, when the electrons are prepared in the form of wave packets, the presence of a quantizing magnetic field B has very important effects on ZB. (1) For $B \neq 0$ the ZB oscillations are permanent while for $B = 0$ they are transient. (2) For $B \neq 0$ many ZB frequencies appear while for $B = 0$ only one frequency is at work. (3) For $B \neq 0$ both interband and intraband (cyclotron) frequencies contribute to ZB while for $B = 0$ there are no intraband frequencies. (4) Magnetic field intensity changes not only the ZB frequencies but the entire character of ZB spectrum. An emission of electromagnetic dipole radiation by the trembling electrons was proposed and described. It was argued that graphene in a magnetic field is a promising system for an experimental observation of Zitterbewegung.

Let us study the ZB effect for massless Dirac fermions in an electromagnetic field and discuss what will add an electric field to the results presented in [22]. In doing so, we describe the dynamics of the system under consideration through the Heisenberg picture. Indeed, we calculate the time evolution of the Dirac position operator

$$\vec{x}(t) = e^{-\frac{i}{\hbar}H_D t}\ \vec{x}\ e^{\frac{i}{\hbar}H_D t} \tag{50}$$

which satisfies the Heisenberg equation of motion

$$\frac{d\vec{x}}{dt} = \frac{i}{\hbar}[H_D, \vec{x}] = v_F\vec{\sigma}_j \tag{51}$$

where H_D is the Hamiltonian given in (1). To get the explicit form of $\vec{x}(t)$, we introduce the dynamics of the Pauli operators

$$-i\hbar\frac{d\vec{\sigma}_j}{dt} = [H_D, \vec{\sigma}_j] \tag{52}$$

which can be evaluated by using the anti-commutation relations $\{\sigma_i, \sigma_j\} = 2\delta_{ij}\mathbb{I}$ $(i, j = x, y, z)$. This leads to the equation

$$-i\hbar\frac{d\vec{\sigma}_j}{dt} = -2v_F\vec{\pi}_j - 2eEy\delta_{yj} + 2H_D\vec{\sigma}_j. \tag{53}$$

It is convenient for later use to introduce the compact form

$$-i\hbar\frac{d\vec{\sigma}_j}{dt} = 2H_D\vec{\eta} \tag{54}$$

where the operator η is given by

$$\vec{\eta} = \vec{\sigma}_j - v_F H_D^{-1}\vec{\pi}_j - eEyH_D^{-1}\delta_{yj} \tag{55}$$

and satisfies the following dynamics

$$-i\hbar\frac{d\vec{\eta}_j}{dt} = -i\hbar\frac{d\vec{\sigma}_j}{dt} = 2H_D\vec{\eta}. \tag{56}$$

It can be solved easily to find

$$\vec{\eta}(t) = e^{\frac{2i}{\hbar}H_D t}\vec{\eta}_0 \tag{57}$$

where $\vec{\eta}_0$ is a constant operator

$$\vec{\eta}_0 = \vec{\eta}(0) = \vec{\sigma}_j(0) - v_F H_D^{-1}\vec{\pi}_j - eEyH_D^{-1}\delta_{yj}. \tag{58}$$

Since we have $\{H_D, \vec{\eta}\} = 0 = \{H_D, \vec{\eta}_0\}$, thus (57) rewrites as

$$\vec{\eta}(t) = \vec{\eta}_0 e^{\frac{2i}{\hbar}H_D t}. \tag{59}$$

Combining (53), (55) and (59), to end up with

$$\frac{d\vec{x}}{dt} = v_F^2 H_D^{-1}\vec{\pi}_j + eEv_F yH_D^{-1}\delta_{yj} + v_F\vec{\eta}_0 e^{-\frac{2i}{\hbar}H_D t} \tag{60}$$

which can be integrated to get the time evolution

$$\vec{x}(t) = v_F^2 H_D^{-1}\vec{\pi}_j t + eEv_F yH_D^{-1}\delta_{yj}t + \frac{1}{2}i\hbar v_F\vec{\eta}_0 H_D^{-1}e^{-\frac{2i}{\hbar}H_D t} + \vec{x}(0) \tag{61}$$

where $\vec{x}(0)$ is a constant (operator) of integration

$$\vec{x}(0) - \frac{1}{2}i\hbar v_F\vec{\sigma}_j(0)H_D^{-1} + \frac{1}{2}i\hbar v_F^2 H_D^{-2}\vec{\pi}_j + \frac{1}{2}i\hbar v_F eEyH_D^{-2}\delta_{yj}. \tag{62}$$

Now using the correspondence (35), which is linking our system with atoms in quantum optics, we map (61) as

$$\begin{aligned}\vec{x}(t) &= \vec{x}(0) + \frac{2\eta^2 l_B^2\Omega^2\vec{\pi}_j + \sqrt{2}eE\eta l_B\Omega y\delta_{yj}}{H_D}t \\ &+ \left(\vec{\sigma}_j(t) - \frac{\sqrt{2}\eta l_B\Omega\vec{\pi}_j + eEy\delta_{yj}}{H_D}\right)\frac{i\sqrt{2}\hbar\eta l_B\Omega}{2H_D}\left(1 - e^{\frac{2i}{\hbar}H_D t}\right).\end{aligned} \tag{63}$$

This result is showing different contributions originated from different sources. Indeed, the first two terms on the r.h.s. account for the classical kinematics of a free particle in electromagnetic field $(\vec{E}, \vec{B})$. However, the last term represents a quantum oscillation about the classical motion with a frequency $\frac{2|E_D|}{\hbar}$ where $E_D = \varepsilon_n$. This oscillating term is the so-called ZB effect or "trembling motion" and its frequency associated with the measurable quantity $\langle \vec{x}(t) \rangle$ can be estimated as

$$\omega_{ZB} = \frac{2|E_D|}{\hbar} = 2\sqrt{4\eta^2\Omega^2|n| + \delta^2} \tag{64}$$

where the correspondence (35) is used. On the other hand, the presence of the electric field $\vec{E}$ is clearly shown in equation (63). Thus, one can interpret the terms $\left(\sqrt{2}eE\eta l_B \Omega y \delta_{yj}\right)$ and $(eEy\delta_{yj})$ as shift with respect to the original terms, which of course disappear if we require $\vec{E} = 0$. This tells us that our results are interesting and generals such that one can recover the standard ones by simply fixing some parameters.

6 Conclusion

The solutions of the energy spectrum of a system of massless Dirac fermions in the electromagnetic field are obtained. The corresponding Dirac Hamiltonian H_D is used to investigate two-level atom interacting with a single electromagnetic field. The connection between JC model in quantum optics with H_D is established in a simple manner without taking any limit on the strength of the electromagnetic field. This can be served as a tool to study atomic transitions in quantum optics using the relativistic quantum mechanical models in the presence of the electromagnetic field.

More precisely, after mapping the eigenspinors in terms of ground and excite states of two-level atom, we derived a new form of the Dirac Hamiltonian. This is used to establish a link with JC and AJC models as linear combination under the correspondence between their parameters. Making a suitable choose of the involved parameters in the game, we showed that the linear combination can be reduced either to the Rashba or Dresselhous couplings. This is a significant results because it relies two sectors such graphene and quantum optic systems.

Because of the Rabi oscillations are occurring in the JC model and its relation to our system, we analyzed them. In fact, we mapped the eigenspinors in terms of two level atom states, i.e. ground and excited and showed that the Rabi frequency can be obtained in terms of the quantized energy levels. Calculating the probabilities for atom in ground and excited states, separately, we obtained different results showing that these probabilities are maximum when the detuning δ is null and decrease rapidly as δ increases. These are used to discuss the resonant case by evaluating the atomic inversion $W(t)$ and conclude that the population of the state is depending on the value attributed to $W(t)$.

Finally, we analyzed the Zeitterbewegung effect for massless Dirac fermions in the electromagnetic field. This was done by using the Heisenberg picture dynamics to evaluate the time evolution of the Dirac position operator. This allowed us to obtain a quantum oscillation about the classical motion with a defined frequency. Its oscillation between the negative and positive energy states is similar to the Rabi oscillation in the two-level atom. By evaluating the position average, we obtained the ZB frequency in terms of the quantized energy system.

We close this part by listing some ideas, which can be worked by adopting our approach presented in this paper. Indeed, it will be of interest to analyze the massless Dirac fermions in the presence of

a perpendicular magnetic field and by considering an electric field supported by 2×2 unit matrix as formulated for graphene in [3]. This certainly will bring new results and interesting conclusions due to the reduction of the magnetic field from B to $B' = B\sqrt{1 - \left(\frac{E}{V_F B}\right)^2}$. One also can study in this framework the tilted magnetic field case instead of an uniform one.

Acknowledgment

The generous support provided by the Saudi Center for Theoretical Physics (SCTP) is highly appreciated by AJ and AEM. AJ acknowledges partial support by King Faisal University. The authors are indebted to the referees for their instructive comments.

References

[1] K.S. Novoselov *et al.*, *Science* **306** (2004) 666.

[2] See, e.g. A.H. Castro Neto *et al.*, *Rev. Mod. Phys.* **81** (2009) 109.

[3] For a recent review see, M.O. Goerbig, *Rev. Mod. Phys.* **83** (20011) 1193.

[4] K.S. Novoselov *et al.*, *Nature* **438** (2005) 197.

[5] Y. Zhang *et al. Nature* **438** (2005) 201.

[6] B. Dora *et al.*, *Phys. Rev. Lett.* **102** (2009) 036803.

[7] E.G. Mishchenko, *Phys. Rev. Lett.* **103** (2009) 246802.

[8] E.T. Jaynes and F.W. Cummings, *Proc. IEEE.* **51** (1963) 89; B.W. Shore and P.L. Knight, *J. Mode. Opt.* **40** (1993) 1195; S.B. Zheng, *Phys. Rev.* **A 77** (2008) 045802.

[9] P. Bertet *et al.*, *Phys. Rev. Lett.* **88** (2002) 143601.

[10] S. Osnaghi *et al.*, *Phys. Rev. Lett.* **87** (2001) 037902.

[11] C. Monroe *et al.*, *Phys. Rev. Lett.* **75** (1995) 4714.

[12] G. Rempe and H. Walther, *Phys. Rev. Lett.* **58** (1987) 353. C.A. Blockey, D.F. Walls and H. Risken, *Europhys. Lett.* **17** (1992) 509; J.I. Cirac *et al.*, *Phys. Rev.* **A 49** (1994) 1202.

[13] C.A. Blockey, D.F. Walls and H. Risken, *Europhys. Lett.* **17** (1992) 509.

[14] D. Leibfried *et al.*, *Rev. Mod. Phys.* **75** (2003) 281.

[15] L. Lamata *et al. Phys. Rev. Lett.* **98** (2007) 253005.

[16] R. Gerritsma *et al. Nature* **463** (2010) 68.

[17] J. Casanova *et al.*, *Phys. Rev.* **A 82** (2010) 020101.

[18] R. Gerritsma *et al.*, *Phys. Rev. Lett.* **106** (2011) 060503.

[19] L. Lamata *et al.*, *New J. Phys.* **13** (2011) 095003.

[20] A Bermudez, M.A. Martin-Delgado and E.Solano, *Phys. Rev.* **A 76** (2007) 041801(R).

[21] M.I. Katsnelson, Eur. Phys. J. **B 51** (2006) 157.

[22] T.M. Rusin and W. Zawadzki, *Phys. Rev.* **B 78** (2008) 125419.

[23] R. Roldan, J.-N. Fuchs and M.O. Goerbig, *Phys. Rev.* **B 82** (2010) 205418.

[24] J. Schliemann, J.C. Egues and D. Loss, *Physica Status Solidi (c)* **3** (2006) 4330.